bulletin 46

state-of-art report

fib
CEB-FIP

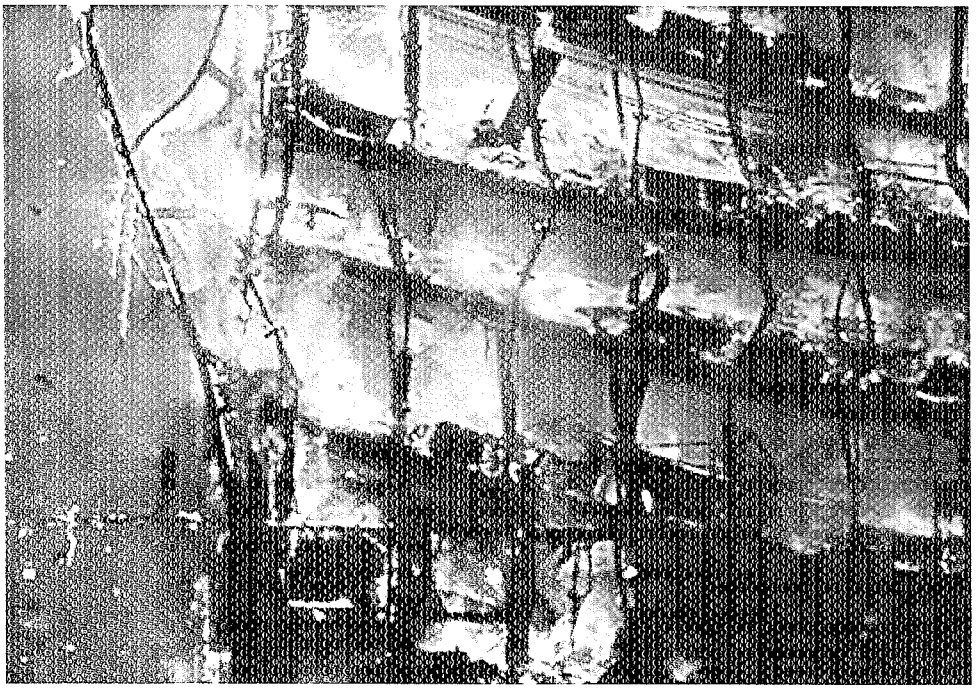

Fire design of concrete structures – structural behaviour and assessment

Fire design of concrete structures – structural behaviour and assessment

State-of-art report prepared by

Task Group 4.3

July 2008

Subject to priorities defined by the Technical Council and the Presidium, the results of *fib*'s work in Commissions and Task Groups are published in a continuously numbered series of technical publications called 'Bulletins'. The following categories are used:

category	minimum approval procedure required prior to publication
Technical Report	approved by a Task Group and the Chairpersons of the Commission
State-of-Art Report	approved by a Commission
Manual, Guide (to good practice) or Recommendation	approved by the Technical Council of *fib*
Model Code	approved by the General Assembly of *fib*

Any publication not having met the above requirements will be clearly identified as preliminary draft.

This Bulletin N° 46 was approved as an *fib* state-of-art report by Commission 4 in May 2008.

This report was drafted by Working party 4.3-2 of Task Group 4.3, *Fire design of concrete structures*, in Commission 4, *Modelling of structural behaviour and design*:

Luc Taerwe (Convener, Ghent University, Belgium)
Patrick Bamonte (Politecnico di Milano, Italy), Kees Both (TNO, the Netherlands), Jean-François Denoël (Febelcem, Belgium), Ulrich Diederichs (Univ. Rostock, Germany), Jean-Claude Dotreppe (Univ. de Liège, Belgium), Roberto Felicetti (Politecnico di Milano, Italy), Joris Fellinger (until 2005), Jean-Marc Franssen (Univ. de Liège, Belgium), Pietro G. Gambarova (Politecnico di Milano, Italy), Niels Peter Høj (HOJ Consulting GmbH, Switzerland), Tom Lennon (BRE, United Kingdom), Alberto Meda (Univ. of Bergamo, Italy), Yahia Msaad (CERIB, France), Josko Ožbolt (Univ. Stuttgart, Germany), Goran Periškić (Univ. Stuttgart, Germany), Paolo Riva (Univ. di Bergamo, Italy), Fabienne Robert (CERIB, France), Arnold Van Acker (Belgium)

Full address details of Task Group members may be found in the *fib* Directory or through the online services on *fib's* website, www.fib-international.org.

Cover image: The Windsor building in Madrid, during the fire in February 2005 (source Calavera et al., 2005; see chapter 7)

First published in 2008 by the International Federation for Structural Concrete (*fib*)
Postal address: Case Postale 88, CH-1015 Lausanne, Switzerland
Street address: Federal Institute of Technology Lausanne - EPFL, Section Génie Civil
Tel +41 21 693 2747 • Fax +41 21 693 6245
fib@epfl.ch • www.fib-international.org

ISSN 1562-3610
ISBN 978-2-88394-086-4

Printed by DCC Document Competence Center Siegmar Kästl e.K., Germany

ISSN 1562-3610
ISBN 978-2-88394-086-4

Fire design of concrete structures – structural behaviour and assessment

Contents

fib CEB-FIP

fédération internationale du béton
International Federation for Structural Concrete
www.fib-international.org

5 Plastic analysis of continuous beams*

5.1 Introduction

It is stated in Eurocode 2 (EN 1992-1-2, 2004 that is an important question is whether load redistributions between different sections of a member in bending can be accepted in case of fire, these redistributions being allowed by the plastic behaviour of both the reinforcement and the concrete. One of the key condition for this plastic behaviour is the ductility of the section, i.e. the capacity of the section to keep on developing the plastic bending moment, when the curvature increases to very high values. This seems to be the case according to some numerical examples that show how the ductility of a section tends to increase during a fire. For instance, the moment-curvature diagrams of a 160x400mm rectangular concrete section heated on three sides are plotted in Fig. 5-1. Four curves are presented, namely at time t = 0', 30', 60' and 90' of ISO 834 fire. In each case, a linear (L) and a nonlinear (NL) descending branch has been considered for concrete stress-strain diagram, with hardly any difference between the two; the nonlinear formulation yields a slightly higher ductility than the linear formulation. Note that the ductility increases significantly in a fire situation, as also observed in a 140 mm-thick slab, where ductility increased much less than in beams.

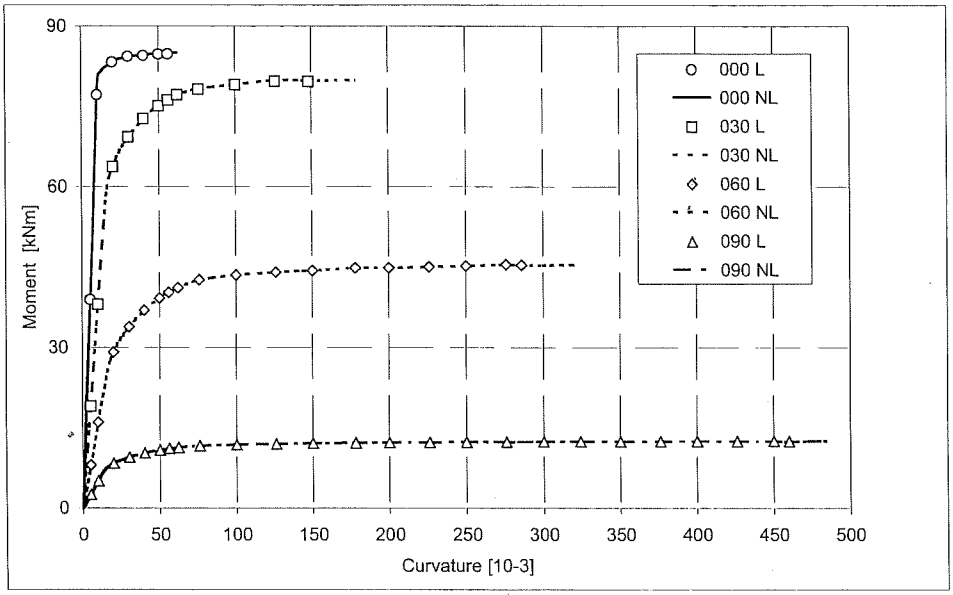

Fig. 5-1: Moment-curvature diagrams of a rectangular section subjected to ISO 834 fire

The main difference between the hot and cold situations is the ratio between the ultimate plastic moment and the first-yielding moment. This ratio is much higher in fire, which means that much higher rotations have to take place before the full plastic moment is reached. This is in no contradiction with what is generally observed during the laboratory tests, where the failure of R/C structures is often accompanied by very large displacements.

The theory of plasticity gives a theoretical validation to the fact that several effects leading to self-equilibrated stress distributions can be neglected in nonlinear numerical analysis. Among these effects, (a) those occurring either in the construction phases or during the service life at room temperature, before the fire starts (due for instance to shrinkage, creep and thermal strains), and (b) those occurring during the fire (due to creep and thermal expansion) should be mentioned. A consequence of neglecting these effects is that the strains,

* by Jean-Marc Franssen and Paolo Riva

stresses and tangent moduli that are computed in any given point of a structure are only approximate – or "mean" – values compared to the "true" values that would be computed if all these effects were taken into account. The computed values are indeed based on the hypothesis of a virgin initial stress distribution, which is far from reality.

Neglecting these self-equilibrated stress distributions is subjected to some limitations, since it is justified as long as the ensuing displacements are small. This is why the effects of thermal expansion during the fire must be taken into account. The thermal strains can indeed reach values up to 1% in steel and up to 1.4 % in concrete, these values being higher or of the same order of magnitude of those occurring at the peak stress, depending on the temperature.

Another strain component that may affect deformations – second-order effects included – in concrete structures submitted to fire is the transient-creep strain. Whether this component has to be taken into account explicitly or implicitly is still a subject of debate. In the stress-strain relationships presented in Eurocode 2, for example, transient-creep strains are incorporated implicitly. Possible reasons why this apparently very simplified model yields reasonable results are:

- the behaviour of a concrete structure is mainly dictated by the behaviour of the steel bars, not by the behaviour of concrete;
- transient creep is not absent from the afore-mentioned simplified model, since it is introduced in an implicit manner;
- an explicit transient-creep model leads to different predictions compared to a simple implicit model only when the material exhibits strain reversals or - more importantly - when the temperature decreases.

These, plus the advantage of utilising a single, widely adopted general model, are probably the reasons why the simple concrete model of Eurocode 2 is so popular among the designers in spite of its many limits.

Nevertheless, it should be noted that the evolution of the strain at the peak stress proposed in the ENV version of Eurocode 2 has been found to be too stiff for representing transient creep. In the revised EN version, the concrete model has been made somehow softer, in order to improve the prediction of the deformations.

5.2 Use of plastic analysis

The objective of plastic analysis is generally to evaluate the load-carrying capacity of a beam. In the following, the fire resistance (R) of the beams analysed in Chapter 3 (concerning the parametric study of continuous beams) is verified by means of Plastic Analysis for a 120' fire duration.

With reference to Fig. 5-2, according to plastic analysis the verification is positive if the ultimate load at the requested fire duration is larger than the applied load, at the onset of beam collapse because of the formation of a suitable number of plastic hinges.

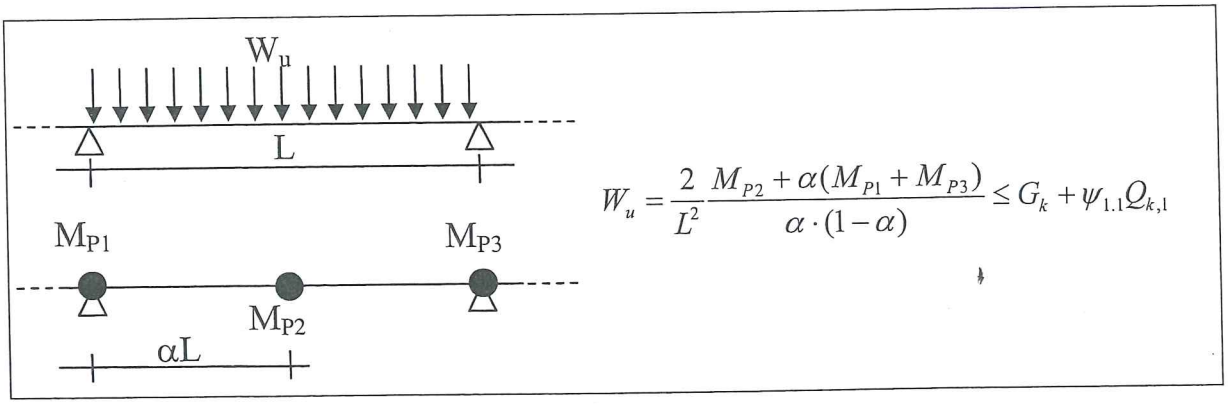

$$W_u = \frac{2}{L^2}\frac{M_{P2} + \alpha(M_{P1} + M_{P3})}{\alpha \cdot (1-\alpha)} \le G_k + \psi_{1.1} Q_{k,1}$$

Fig. 5-2: Verification by means of Plastic Analysis

The plastic (e.g. ultimate) moments at critical sections may be determined according to various sectional-analysis method, such as the constant-isothermal method or the zone method, both suggested by EC2.

In axially-unrestrained beams, the application of plastic analysis is straightforward and generally leads to a conservative estimate of the ultimate load.

In case of axially-restrained beams, the ultimate bending-moment value depends on the axial force developed during the fire. Accordingly, the axial-force value has to be estimated prior to sectional analysis, based on fire effects and on the actual axial restraint of the beam.

An approximate estimate of the axial force, to be adopted in plastic analysis, can be performed via the simplified procedure outlined below and shown in Fig. 5-3 (Riva, 2005):

- based on the results of the thermal analysis after a time t of exposure to the fire, the average temperature distribution at each level along the section is determined as shown in Fig. 5-3a and the average temperature in the section is found, as shown in Fig. 5-3b;
- the axial force ensuing from the restrained thermal elongation under a constant temperature distribution is evaluated by computing the normal stress σ_{th} arising in a beam of stiffness $K_{beam} = (E_{\Delta T,ave}A)/l$, axially restrained by a spring of stiffness $K = k(E_{C,20°C}A)/l$, as a consequence of an average thermal elongation $\varepsilon_{T,Ave}$, and multiplying such a stress by 0.30A, A being the cross-section area of the beam (Figs. 5-3c and d). The value of the axial force determined in this way has been checked against the results of the nonlinear parametric analysis (Chapter 3) and has been found to be - in most cases - acceptable for design purposes.
- the plastic (i.e. ultimate) moments of the critical sections are determined by means of either the 500°C-isotherm method or the zone method (CEN 2005, Anderberg and Thelandersson 1976), considering also the axial force.

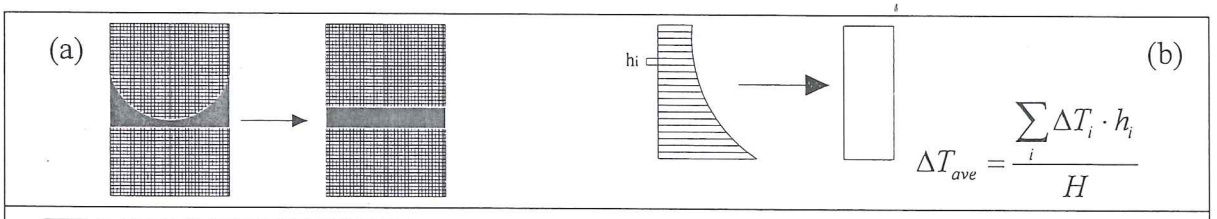

$E_{C,20°C}$	Young's modulus of concrete at ambient temperature
$E_{\Delta Tave}$	Young's modulus of concrete at average section temperature after t min. of fire exposure
$\varepsilon_{T,Ave}$	average thermal strain
σ_{th}	axial stress arising from the axial restraint due to thermal strain $\varepsilon_{c,\Delta Tave}$
ΔT_{ave}	average temperature due to fire after t min. of fire exposure (Fig. 5-3b)

Fig. 5-3: Evaluation of the axial force in axially-restrained beams

The results of the plastic analysis verification after 120' of exposure to a standard ISO 834 fire for the same set of single-span, clamped-end beams analysed in the parametric study is presented in Tables 1 to 6, where reference is made also to the results obtained by means of nonlinear analysis (Chapter 4). In the plastic analysis, the section capacity has been determined by means of the 500°C isothermal method. On the basis of the results shown in the afore-mentioned tables, the following comments can be made:

- in the case of no axial restraint (K=0), the ultimate bending capacity of the critical sections at any given fire duration is generally underestimated. As a result, plastic analysis underestimates the ultimate load-carrying capacity of a beam, thus leading to conservative results;
- the assumed axial force in axially-restrained beams results in a lower-bound estimate of the actual force (as given by nonlinear analysis). Hence, the proposed method underestimates the effects of the axial restraint;
- in most cases, the ultimate bending moment of fully axially-restrained beams is overestimated, particularly close to the end sections. As a result, plastic analysis leads - in most cases - to a non-conservative estimate of the ultimate load-carrying capacity. In the case of the fully- restrained 6m-span T-beam, plastic analysis leads to the conclusion that, after a 120'fire duration, the beam is still able to carry a load equal to 90.3 kN/m, while the collapse occurs earlier on the basis of nonlinear analysis.
- for partially-restrained beams, plastic analysis leads in most cases to acceptable results, i.e. to conservative results or to slightly non-conservative results.

Though the results of plastic analysis demonstrate that the safety of a beam at a given fire duration can be assessed rather easily also in axially-restrained beams, one should observe that the proposed method is affected by some rather crude approximations, for example (a) in the estimate of the axial force due to the axial restraint, and (b) in the choice of the effective section (enveloped by the 500°C-isothermal line). These assumptions may lead to some non-conservative results.

However, it is observed that in plastic analysis, by completely neglecting the effects of the axial restraint, the estimate of the ultimate load-bearing capacity of a beam is always on the safe side.

Table 5-1: Results of the plastic-analysis for a 6m beam with rectangular section

Time t=120' – Average Temperature ΔT_{ave} = 383.9°C

B [mm]	H[mm]	$E_{c,20°C}$ [MPa]	A_{s1} [mm²]	T_{As1} [°C]	A_{s2} [mm²]	T_{As2} [°C]
350	500	18 000	628	492.0	628	108.7
B_{red} [mm]	H_{red} [mm]	$E_{c,120'}$ [MPa]	A_{sinf} [mm²]	TA_{sinf} [°C]		$\varepsilon_{T,Ave}$
295	445	5 982.7	628	746.9		4.58E-03

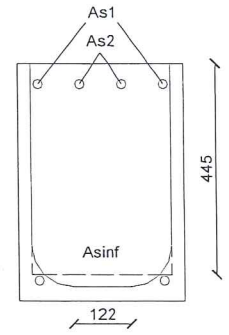

Mid-Span: $A_{s2} = 0$

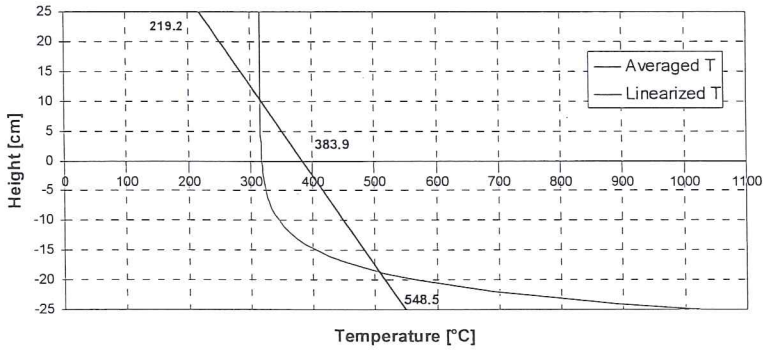

Plastic Moments at Critical Sections (Anderberg's method vs. Non-Linear Analysis)

Restraint	*σ*	N_{th}	N_{an}	*Error*	M^+_{pl}	M^+_{an}	*Error*	M^-_{pl}	M^-_{an}	*Error*
	[MPa]	*[kN]*	*[kN]*	*[%]*	*[kNm]*	*[kNm]*	*[%]*	*[kNm]*	*[kNm]*	*[%]*
K=0	0.0	0.0	0.0	0.0	14.4	36.6	-60.5	186.4	180.6	3.2
K=EA/3L	13.71	719.7	1021.0	-29.5	185.8	203.6	-8.8	298.4	244.1	22.2
K=EA/L	20.55	1078.7	1406.0	-23.3	238.4	229.1	4.0	286.1	231.5	23.6
K=∞	27.38	1437.2	1803.0	-20.3	254.0	234.6	8.3	247.7	201.2	23.1

Plastic Analysis – $\{W_u = (M^-_{pl} + M^+_{pl}) \cdot 8/L^2 \geq W = 42$ kNm$\}$

K=0	*K=EA/3L*	*K=EA/L*	*K=∞*
W_u = 44.6 kNm	W_u = 107.6 kNm	W_u = 116.6 kNm	W_u = 111.5 kNm
$W_{u,NLA}$ = 48.3 kNm	$W_{u,NLA}$ = 99.5 kNm	$W_{u,NLA}$ = 102.3 kNm	$W_{u,NLA}$ = 96.8 kNm

Table 5-2: Plastic analysis data and results for the 6m span T-beam

Time t=120' – Average Temperature ΔT_{ave} = 442.5°C

B [mm]	H[mm]	$E_{c,20°C}$ [MPa]	A_{ssup} [mm²]	T_{Assup} [°C]	A_{s1inf} [mm²]	T_{As1inf} [°C]
1000	400	18 000	1570	95.0	628	690.0
B_{red} [mm]	H_{red} [mm]	$E_{c,120'}$ [MPa]	A_{s2inf} [mm²]	TA_{s2inf} [°C]		$\varepsilon_{T,Ave}$
1000	349	4 385.7	314	620.0		5.80E-03

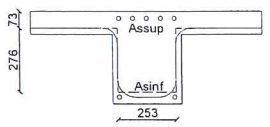

End Sections

$A_{ssup} = 1570mm^2$

$A_{sinf} = 628mm^2$

Mid-Span:

$A_{ssup} = 628mm^2$

$A_{sinf} = 942mm^2$

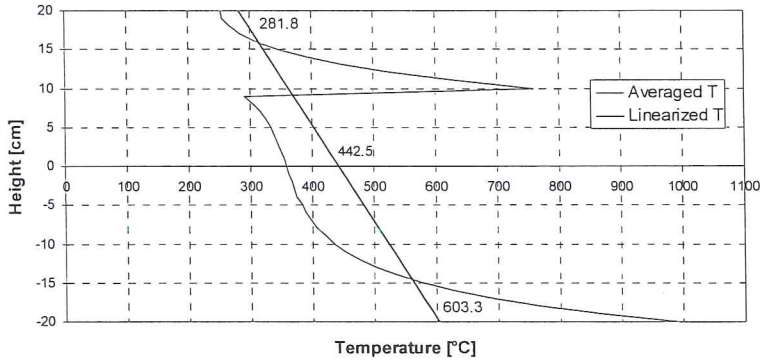

Plastic Moments at Critical Sections (Anderberg's method vs. Non-Linear Analysis)

Restraint	*σ*	N_{th}	N_{an}	*Error*	M^+_{pl}	M^+_{an}	*Error*	M^-_{pl}	M^-_{an}	*Error*
	[MPa]	*[kN]*	*[kN]*	*[%]*	*[kNm]*	*[kNm]*	*[%]*	*[kNm]*	*[kNm]*	*[%]*
K=0	0.0	0.0	0.0	0.0	46.6	54.3	-14.2	201.5	212.8	-5.3
K=EA/3L	14.7	837.0	1295.0	-35.4	210.1	241.8	-13.1	164.0	111.3	47.4
K=EA/L	20.4	1164.9	1753.0	-33.5	266.8	300.2	-11.1	129.3	53.9	139.8
K=∞	25.4	1448.8	-	-	312.9	-	-	93.7	-	-

Plastic Analysis – $\{W_u = (M^-_{pl} + M^+_{pl}) \cdot 8/L^2 \geq W = 42$ kNm$\}$

K=0	*K=EA/3L*	*K=EA/L*	*K=∞*
W_u = 55.1 kNm	W_u = 83.1 kNm	W_u = 88.0 kNm	W_u = 90.4 kNm
$W_{u,NLA}$ = 59.4 kNm	$W_{u,NLA}$ = 78.5 kNm	$W_{u,NLA}$ = 78.7 kNm	$W_{u,NLA}$ = Collapsed

Table 5-3: Results of the plastic analysis for a 6m one-way slab

Time t=120' – Average Temperature ΔT_{ave} = 229.0°C

B [mm]	H[mm]	$E_{c,20°C}$ [MPa]	$A_{ss,end}$ [mm²]	$A_{si,end}$ [mm²]	TA_{sinf} [°C]	T_{Assup} [°C]
1250	250	18 000	678	6784	463.0	29.0
B_{red} [mm]	H_{red} [mm]	$E_{c,120'}$ [MPa]	$A_{ss,mid}$ [mm²]	$A_{si,mid}$ [mm²]		$\varepsilon_{T,Ave}$
1250	220	10 222.0	678	678		2.16E-03

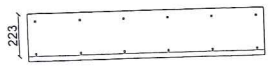

End Sections
$A_{s,sup}$ = 678 mm²
$A_{s,inf}$ = 678 mm²

Mid-Span
$A_{s,sup}$ = 678 mm²
$A_{s,inf}$ = 678 mm²

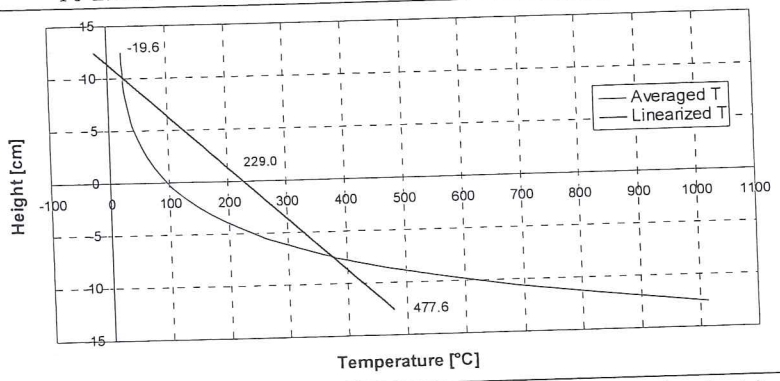

Plastic Moments at Critical Sections (Anderberg's method vs. Non-Linear Analysis)

Restraint	σ	N_{th}	N_{an}	*Error*	M^+_{pl}	M^+_{an}	*Error*	M_{pl}	M_{an}	*Error*
	[MPa]	*[kN]*	*[kN]*	*[%]*	*[kNm]*	*[kNm]*	*[%]*	*[kNm]*	*[kNm]*	*[%]*
K=0	0.0	0.0	0.0	0.0	48.5	70.8	-31.5	59.9	107.6	-44.3
K=EA/3L	8.2	764.4	1148.0	-33.4	143.7	179.7	-20.1	159.6	178.1	-10.4
K=EA/L	14.1	1318.2	1610.0	-18.1	182.6	215.8	-15.4	199.7	195.3	2.2
K=∞	22.0	2066.7	2222.0	-7.0	213.4	252.2	-15.4	228.0	208.9	9.1

Plastic Analysis – $\{W_u = (M^-_{pl} + M^+_{pl}) \cdot 8/L^2 \geq W = 11.56$ kNm$\}$

K=0	*K=EA/3L*	*K=EA/L*	*K=∞*
W_u = 24.1 kNm	W_u = 67.4 kNm	W_u = 85.0 kNm	W_u = 98.1 kNm
$W_{u,NLA}$ = 39.6 kNm	$W_{u,NLA}$ = 79.5 kNm	$W_{u,NLA}$ = 91.4 kNm	$W_{u,NLA}$ = 102.5 kNm

Table 5-4: Results of the plastic analysis for a 9m beam with rectangular section

Time t=120' – Average Temperature ΔT_{ave} = 250.2°C

B [mm]	H[mm]	$E_{c,20°C}$ [MPa]	A_{s1} [mm²]	T_{As1} [°C]	A_{s2} [mm²]	T_{As2} [°C]
550	700	18 000	628	463.0	1570	98.0
B_{red} [mm]	H_{red} [mm]	$E_{c,120'}$ [MPa]	A_{sinf} [mm²]	TA_{sinf} [°C]		$\varepsilon_{T,Ave}$
494	698	9 591.7	628/942	702.9/472.0		2.43E-03

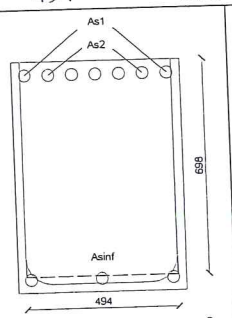

Mid-Span: A_{s2} = 0
A_{sinf} = 1570mm²

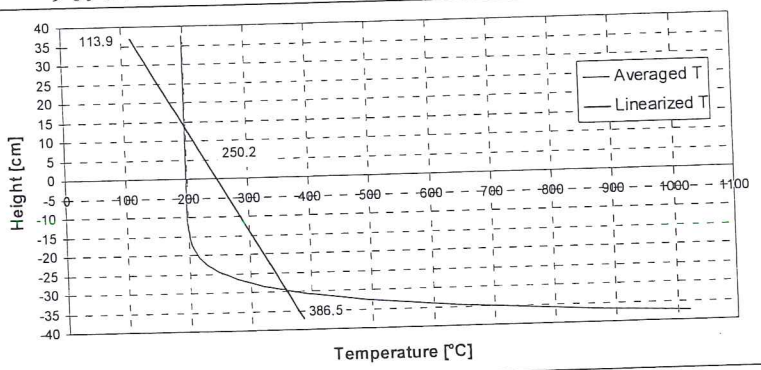

Plastic Moments at Critical Sections (Anderberg's method vs. Non-Linear Analysis)

Restraint	σ	N_{th}	N_{an}	*Error*	M^+_{pl}	M^+_{an}	*Error*	M_{pl}	M_{an}	*Error*
	[MPa]	*[kN]*	*[kN]*	*[%]*	*[kNm]*	*[kNm]*	*[%]*	*[kNm]*	*[kNm]*	*[%]*
K=0	0.0	0.0	0.0	0.0	282.4	209.2	35.0	606.3	673.6	-10.0
K=EA/3L	9.0	1110.7	1762.0	-37.0	539.2	677.4	-20.4	892.9	1688.8	-47.1
K=EA/L	15.2	1883.0	2418.0	-22.1	726.7	782.3	-7.1	1039.0	1314.7	-21.0
K=∞	23.3	2886.4	3235.0	-10.8	908.7	867.4	4.8	1164.0	1234.2	-5.7

Plastic Analysis – $\{W_u = (M^-_{pl} + M^+_{pl}) \cdot 8/L^2 \geq W = 63$ kNm$\}$

K=0	*K=EA/3L*	*K=EA/L*	*K=∞*
W_u = 80.4 kNm	W_u = 123.7 kNm	W_u = 172.6 kNm	W_u = 221.3 kNm
$W_{u,NLA}$ = 87.2 kNm	$W_{u,NLA}$ = 233.7 kNm	$W_{u,NLA}$ = 207.1 kNm	$W_{u,NLA}$ = 207.6 kNm

Table 5-5: Results of the plastic analysis for a 9m T-beam

Time t=120' – Average Temperature ΔT_{ave} = 321.8°C

B [mm]	H[mm]	$E_{c,20°C}$ [MPa]	A_{ssup} [mm^2]	T_{Assup} [°C]	A_{s1inf} [mm^2]	T_{As1inf} [°C]
1350	750	18 000	2198	95.0	628	690.0
B_{red} [mm]	H_{red} [mm]	$E_{c,120'}$ [MPa]	A_{s2inf} [mm^2]	TA_{s2inf} [°C]		$\varepsilon_{T,Ave}$
1350	693	7 017.0	942	620.0		3.48E-03

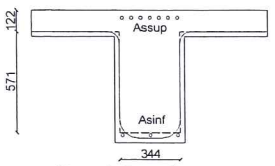

End Sections
A_{ssup} = 2198mm^2
A_{sinf} = 942mm^2
Mid-Span:
A_{ssup} = 628mm^2
A_{sinf} = 1570mm^2

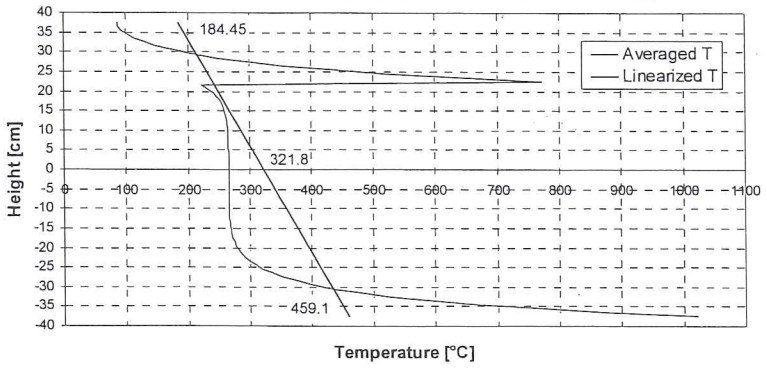

Plastic Moments at Critical Sections (Anderberg's method vs. Non-Linear Analysis)

Restraint	σ [MPa]	N_{th} [kN]	N_{an} [kN]	*Error* [%]	M^+_{pl} [kNm]	M^+_{an} [kNm]	*Error* [%]	M^-_{pl} [kNm]	M^-_{an} [kNm]	*Error* [%]
K=0	0.0	0.0	0.0	0.0	212.1	243.0	-12.7	640.5	809.0	-20.8
K=EA/3L	11.3	1495.2	2258.0	-33.8	659.1	979.8	-32.7	675.4	867.4	-22.1
K=EA/L	17.6	2334.0	3127.0	-25.4	887.4	1236.8	-28.3	537.6	752.6	-28.6
K=∞	24.4	3243.9	4221.0	-23.1	1109.0	1529.3	-27.5	365.1	497.1	-26.6

Plastic Analysis – {$W_u = (M^-_{pl} + M^+_{pl})\cdot 8/L^2 \geq W$ = 63 kNm}

K=0	*K=EA/3L*	*K=EA/L*	*K=∞*
W_u = 84.2 kNm	W_u = 131.8 kNm	W_u = 140.7 kNm	W_u = 145.6 kNm
$W_{u,NLA}$ = 103.9 kNm	$W_{u,NLA}$ = 182.4 kNm	$W_{u,NLA}$ = 196.5 kNm	$W_{u,NLA}$ = 200.1 kNm

Table 5-6: Plastic analysis data and results for the 9m span one-way slab

Time t=120' – Average Temperature ΔT_{ave} = 177.8°C

B [mm]	H[mm]	$E_{c,20°C}$ [MPa]	$A_{ss,end}$ [mm^2]	$A_{si,end}$ [mm^2]	TA_{sinf} [°C]	T_{Assup} [°C]
1400	350	18 000	1608	1206	473.0	23.0
B_{red} [mm]	H_{red} [mm]	$E_{c,120'}$ [MPa]	$A_{ss,mid}$ [mm^2]	$A_{si,mid}$ [mm^2]		$\varepsilon_{T,Ave}$
1400	296	12 037.7	1206	1206		1.55E-03

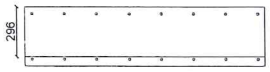

End Sections
$A_{s,sup}$ = 4870 mm^2
$A_{s,inf}$ = 1963 mm^2

Mid-Span
$A_{s,sup}$ = 452 mm^2
$A_{s,inf}$ = 3927 mm^2

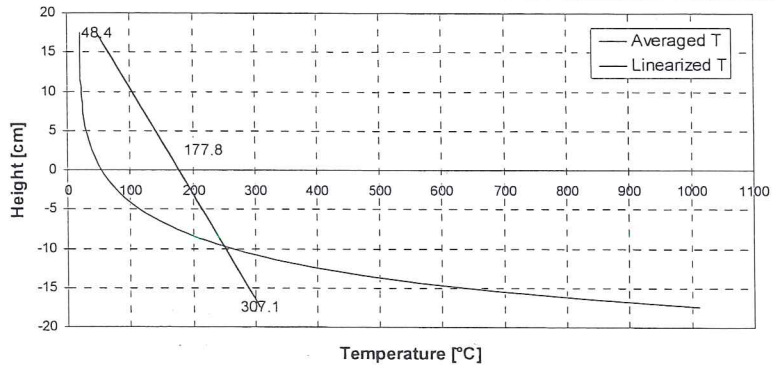

Plastic Moments at Critical Sections (Anderberg's method vs. Non-Linear Analysis)

Restraint	σ [MPa]	N_{th} [kN]	N_{an} [kN]	*Error* [%]	M_{Nth} [kNm]	M^+_{pl} [kNm]	M^+_{an} [kNm]	*Error* [%]	M^-_{pl} [kNm]	M^-_{an} [kNm]	*Error* [%]
K=0	0.0	0.0	0.0	0.0	0.0	111.5	120.3	-7.3	222.0	320.5	-30.7
K=EA/3L	6.2	911.8	1290.0	-29.3	111.7	349.9	308.0	13.6	454.4	439.7	3.3
K=EA/L	11.2	1642.5	1792.0	-8.3	201.2	433.4	373.2	16.1	533.7	473.0	12.8
K=∞	18.6	2741.0	2575.0	6.4	335.8	603.3	465.1	29.7	667.8	516.6	29.3

Plastic Analysis – {$W_u = (M^-_{pl} + M^+_{pl})\cdot 8/L^2 \geq W$ = 16.45 kNm}

K=0	*K=EA/3L*	*K=EA/L*	*K=∞*
W_u = 32.9 kNm	W_u = 79.4 kNm	W_u = 95.5 kNm	W_u = 125.5 kNm
$W_{u,NLA}$ = 43.5 kNm	$W_{u,NLA}$ = 73.8 kNm	$W_{u,NLA}$ = 83.6 kNm	$W_{u,NLA}$ = 97.0 kNm

5.3 Conclusions

The results obtained by means of plastic analysis lead to the following concluding remarks:

- Plastic analysis is a simple and straightforward method, that is very sensitive to the evaluation
  (a) of the plastic moments at the supports, and
  (b) of the effects of the axial restraints.
- Neglecting the effects of the axial restraints always leads to a conservative estimate of the ultimate load- carrying capacity in statically-redundant beams.

The latter observation lead to the conclusion that designing a continuous beam subjected to fire, using plastic analysis, is on the safe side, if the effects of the axial restraints are ignored.

References

Anderberg, Y., and Thelandersson, S. (1976). "Stress and Deformation Characteristics of Concrete at High Temperature – 2. Experimental Investigation and Material Behaviour Model." *Lund Institute of Technology*, August 1976, 84pp.

EN 1992-1-2: "Eurocode 2: Design of Concrete Structures – Part 1-2: General rules – Structural Fire Design", December 2004, 97 pp.

Riva, P. (2005). "Nonlinear and Plastic Analysis of RC Çoncrete Beams." *Proc. Int. Wsorkshop Fire Design of Concrete Structures: What now? What next?*, Milano, 2-4 Dicembre 2004, Starry Link Editore.

Notation

A_s	reinforcing steel area
B	cross section width
B_{red}	reduced cross section width, based on 500°C isothermal method
$E_{c,20°C}$	concrete Young's modulus at 20°C
$E_{c,120'}$	concrete Young's modulus after 120' of fire duration
H	cross section height
H_{red}	reduced cross section height, based on 500°C isothermal method
K	axial restraint of beam
M_{pl}	plastic moment resulting from 500°C isothermal method
M_{an}	ultimate meoment resulting from parametric study (Chapter 4)
N_{th}	axial force due to thermal elongation evaluated as shown in Fig. 5-2
N_{an}	axial force due to thermal elongation resulting from parametric study (Chapter 4)
T_{As}	reinforcing steel temperature
W	load applied to the beam, sum of dead and live load
W_u	ultimate load resulting from plastic analysis
$W_{u,NLA}$	ultimate load resulting from nonlinear analysis (Chapter 4)
ΔT_{ave}	average temperature due to fire after t min. of fire exposure
$\varepsilon_{T,ave}$	average thermal elongation
σ	normal stress due to thermal elongation and axial restraint